Journal of Immunological Methods 467 (2019) 19–28

Contents lists available at ScienceDirect

Journal of Immunological Methods

journal homepage: www.elsevier.com/locate/jim

Optimized protocols for studying the NLRP3 inflammasome and assessment of potential targets of CP-453,773 in undifferentiated THP1 cells

Julia A. Guzova[a,c], Michael J. Primiano[a], Aiping Jiao[a], Jeffrey Stock[b], Chiachin Lee[b], Aaron R. Winkler[a], J. Perry Hall[a,*]

[a] Inflammation & Immunology Research Unit, Pfizer, Cambridge, MA 02139, United States
[b] Department of Discovery Sciences, Pfizer, Groton, CT 06340, United States
[c] Department of Pharmacology & Experimental Therapeutics, Boston University School of Medicine, Boston, MA 02118, United States

ARTICLE INFO

Keywords:
ABCb7
ABCb10
Interleukin-1beta (IL-1β), NLRP3 inflammasome
THP1
CP-456,773

ABSTRACT

The NLRP3 inflammasome is a complex multimeric signaling apparatus that regulates production of the pro-inflammatory cytokine IL-1β. To overcome both the variability among primary immune cells and the limitations of genetic manipulation of differentiated human or murine macrophages, we developed a simplified, reliable and relevant cell-based model for studying the NLRP3 inflammasome using the undifferentiated human myelomonocytic cell line THP1. Undifferentiated THP1 cells constitutively express NLRP3, and NLRP3 inflammasome activation occurred in response to canonical NLRP3 activation stimuli including nigericin, ATP, and urea crystals, culminating in pro-IL-1β cleavage, extracellular release of mature IL-1β, and pyroptosis. We used this THP1 cell system to investigate potential targets of the potent, NLRP3 inflammasome selective inhibitor CP-456,773. We optimized a viral shRNA transduction method for gene expression knockdown (KD), and the KD of NLRP3 itself eliminated inflammasome activation and IL-1β production. NLRP3 inflammasome activation and CP-453,773 pharmacology were not altered in ABCb7- or ABCb10-deficient THP1 cells, eliminating these gene products as candidate pharmacological targets of CP-453,773. For ABCb10, we confirmed our results using CRISPR/CAS9-mediated *ABCb10* knockout (KO) THP1 sub-lines. In summary, undifferentiated THP1 cells are fully competent for activation of the NLRP3 inflammasome and production of IL-1β, without differentiation into macrophages, and we describe optimized KD and KO methodologies to manipulate gene expression in these cells. As an example of the utility of undifferentiated THP1 cells for investigations into the biology of the NLRP3 inflammasome, we have used this cell system to rule out ABCb7 and ABCb10 as potential targets of the NLRP3 inflammasome inhibitor CP-453,773.

1. Introduction

Interleukin-1beta (IL-1β), a pyrogenic and inflammatory cytokine, is released by cells of the innate immune system as a result of a two-step process (Lopez-Castejon and Brough, 2011; Dupont et al., 2011; Piccioli and Rubartelli, 2013; Dinarello, 2015). The transcription and translation of biologically inactive pro-IL-1β is induced by a variety environmental insults, including Toll-like receptor (TLR) ligands such as lipopolysaccharide (LPS), and the inflammatory cytokine TNFα. The exposure of these so-called primed cells to a variety of intrinsic and extrinsic cellular stressors triggers the assembly of a large, intracellular multimeric complex termed the inflammasome. Inflammasomes coordinate caspase-1-dependent processing and cleavage of pro-IL-1β into biologically active IL-1β (Horvath et al., 2011; Vanaja et al., 2015; Place and Kanneganti, 2018). These many secondary stressors all appear to signal *via* a marked reduction in intracellular potassium ion (K^+) levels, which is thought to drive inflammasome assembly (Perregaux et al., 1992; Munoz-Planillo et al., 2013). Among the human inflammasome subtypes, including those mediated by NLRP3, NLRC4, NLRP1 and AIM2, the NOD-like receptor 3 (NLRP3) inflammasome is possibly the most studied and well-characterized, and its activation is implicated in the pathogenesis of many infectious, autoimmune and inflammatory diseases (Berman et al., 2014; Franchi et al., 2009; Place and Kanneganti, 2018). Canonical secondary stressors/stimuli of the NLRP3 inflammasome include: pore-forming toxins; intracellular infection with bacteria, viruses, or fungi; the antibiotic and K^+ ionophore nigericin; and engulfed particulate matter such as silica, cholesterol, and urate crystals (Chavarria-Smith and Vance, 2015; He et al., 2016;

* Corresponding author.
E-mail address: james.p.hall@pfizer.com (J.P. Hall).

https://doi.org/10.1016/j.jim.2019.02.002
Received 14 November 2018; Received in revised form 4 February 2019; Accepted 4 February 2019
Available online 05 February 2019

Duncan and Canna, 2018; Rathinam et al., 2010). In addition, inflammasome activation often leads to the inflammatory form of cell death known as pyroptosis, in which cells releasing IL-1β rupture and ultimately die (Fink and Cookson, 2005; Liu and Lieberman, 2017).

Despite intense investigation, many aspects of NLRP3 inflammasome biology have yet to be elucidated. To advance the understanding of NLRP3 inflammasome activation and function, a simplified and consistent *in vitro* model tolerant of genetic manipulation would be advantageous. The vast majority of *in vitro* research related to NLRP3 inflammasome activation and its inhibition has been performed in mouse cellular systems. The reported studies in human cell systems have utilized primary human macrophages and peripheral blood mononuclear cells (PBMC) as *in vitro* models. NLRP3 protein expression in primary human macrophages requires LPS stimulation, and responses to LPS stimulation are notoriously variable among individual human macrophage donors (Buscher et al., 2017; Longo et al., 2012). Some limitations in mouse macrophage systems include differences in mouse-to-human translation of the threshold dose of the secondary stressor signal required to induce IL-1β release (Wang et al., 2013), and the inherent resistance of mouse cells to lentiviral transduction (Cante-Barrett et al., 2016). An *in vitro* model system based on a stable, proliferating human monocyte cell line would provide an ideal compromise, combining the biological disease relevance of a human cell system with the consistency of genetic manipulation (*i.e.*, KD and KO) in a cell line. Surveying the literature, it is clear that the vast majority of inflammasome research performed in THP1 cells has been done in cells stimulated with phorbol 12-myristate 13-acetate (PMA) to adopt a more macrophage-like phenotype (Zhou et al., 2011; Nomura et al., 2015; Kim et al., 2016). Recently a few investigators have utilized THP1 cells without a PMA pre-treatment step in their investigations of the NLRP3 inflammasome (Cullen et al., 2015; Nagar et al., 2018). We chose to investigate NLRP3 inflammasome biology in the human myelomonocytic THP1 cell line because of its potential as a reproducible and genetically modifiable model of human myeloid cell and inflammasome activation, while acknowledging that there are a number of caveats to consider when selecting a THP1 based model. These include the facts that THP1 contain some chromosomal abnormalities (Adati et al., 2009) and that this cell line does not recapitulate all the functional characteristics of primary macrophages and monocytes (Schildberger et al., 2013; Mukherjee et al., 2018). We reasoned that dispensing with PMA-induced macrophage differentiation would simplify this model system even further.

The Cytokine Release Inhibitory Drug (CRID) series of small molecule inhibitors was originally developed based on a phenotypic screen of inhibitors of LPS plus ATP-induced IL-1β release from human macrophages (Perregaux et al., 2001). CP-453,773, also termed CRID3, and, subsequently, MCC950, (Laliberte et al., 2003; Coll et al., 2015), is a diarylsulfonylurea-containing compound that was ultimately advanced for clinical testing. CP-453,773 does not impact the synthesis of pro-IL-1β, but it potently and selectively inhibits assembly and activation of the NLRP3 inflammasome, and, consequently, the processing of pro-IL-1β to IL-1β (Perregaux et al., 2001; Coll et al., 2015; Primiano et al., 2016). Despite its use by researchers in the field over many years, the precise pharmacological target of CP-453,773 has remained unknown. CP-453,773 is structurally related to the anti-diabetic drug glyburide, which also inhibits NLRP3 inflammasome activation but with significantly lower potency (Lamkanfi et al., 2009). Glyburide binds to SUR1, SUR2a, and SUR2b – encoded by the *ABCc8* and *ABCc9* genes – on the surface of pancreatic β-cells. Glyburide agonizes SUR-mediated antagonism of the inwardly-rectifying ATP-sensitive K^+ (K_{ATP}) channels $K_{ir}6.1$ and $K_{ir}6.2$, resulting in insulin exocytosis. Although it has been shown that CP-456,773 has no insulin secretagogue activity in β-cells (Hill et al., 2017), the structural similarity between CRID3 and glyburide led us to hypothesize that CP-456,773 may bind to a SUR-like protein to effect an inhibition of NLRP3 inflammasome assembly and IL-1β production. Given the importance of mitochondria and mitochondrial functions in NLRP3 inflammasome activation (Zhou et al., 2011; Nakahira et al., 2011; Murakami et al., 2012; Iyer et al., 2013; Subramanian et al., 2013; Gurung et al., 2015), we assessed whether the mitochondrial SUR-like proteins ABCb7 and ABCb10 could be the target(s) of CP-453,773 (Bekri et al., 2000; Yano, 2017).

In the present work, we provide optimized methods for studying the biology of the NLRP3 inflammasome pathway in undifferentiated THP1 cells. We optimized KD and KO methods for THP1 cells, and we validated our system by silencing the receptor protein of the NLRP3 inflammasome, NLRP3 itself. We tested the mitochondrial transporters ABCb7 and ABCb10 in NLRP3 inflammasome activation, and we demonstrated that ABCb7 and ABCb10 are unlikely to be the pharmacologic target(s) of the NLRP3 inflammasome inhibitor CP-453,773.

2. Materials and methods

2.1. Chemicals and reagents

LPS (*Escherichia coli* 0111:B4, cat # L6529) and ATP (cat# GE27-2056-01) were purchased from Sigma (St. Louis, MO). Nigericin was obtained from Tocris (Cat# 4321, Minneapolis, MN); Monosodium Urate Concentrate (cat# tlrl-msu-25; AG-CR1-3950) was from InvivoGen and from AdipoGen respectively (San Diego, CA). Polybrene for THP1 cell transduction was from AmericanBio (cat# AB0164300001, Natick, MA). Puromycin for KD selection was from Gibco Life Technology (cat# A1113803, Frederick, MD). The antibody against IL-1β was from Abcam (Cat# ab2105); antibodies against Caspase-1 (Cat# 4199), NLRP3 (Cat# 15101), β-actin (Cat# 3700) and α-tubulin (Cat# 3873) were from Cell Signaling Technology (Danvers, MA). Detection antibodies for immunoblotting were from Li-Cor Biotechnology: IRDye® 800CW goat anti-rabbit IgG and IRDye®, 680RD goat anti-mouse IgG (cat# 925-32211 and 925-68070). Lentivirus packaging plasmids pMD2.G (pVSV-G) and ps.PAX2 (pPAX) were custom made in bulk by GenScript (Piscataway, NJ). Gene-specific backbone plasmids were on pZIP-SFFV-ZsGreen-Puro backbone from transOMIC technologies (cat# TLMSU1400, Huntsville, AL). For KO generation we used Cell Line Nucleofector Kit V (cat# VCA-1003, Lonza, Walkersville, MD), with TrueCut Cas9 Protein v2 (cat# A36498, Thermo Fisher). Levels of the cytokines IL-1β and TNFα in media were measured on the Meso Scale Discovery platform, according to the manufacturer's instructions (cat# K15052D-2, Rockville, MD). Amicon Ultra-0.5 Centrifugal Filter Devices-10 K columns were from Millipore (cat# UFC501024, Burlington, MA). CP-453,773 (CP-456,773, sodium salt CAS 256373-96-3), was synthesized at Pfizer as previously described (Laliberte et al., 2003). RNA isolation kit was from Qiagen (cat# 74181, Germantown, MD). Odyssey® Blocking Buffer (cat# 927-50003, LiCor, Lincoln, NE) was used in immunoblot experiments. The cellular toxicity assay was done using the LDH kit from Roche (cat #11644793001), and cell viability was assessed by the CellTiter-Glo® Luminescent Assay from Promega (cat# G7571, Madison, WI). Phosphatase and Protease Inhibitor Cocktails were from ThermoFisher Scientific (Cat#78428 and 78,430, respectively, Waltham, MA). Cell culture reagents were from Life Technologies including RPMI-1640 cat# 11875-093 (Frederick, MD).

2.2. Cell culture

The human monocytic cell line THP1 was obtained from ATCC (Manassas, VA, USA). THP1 cells were grown in RPMI-1640 supplemented with 10% heat-inactivated fetal bovine serum, MEM amino acids, 1% Antibiotic-Antimycotic, 10 mM HEPES buffer (Thermo Fisher) at 37 °C/5% CO_2 humidified incubator. For inflammasome activation experiments, RPMI without supplements was used. The LentiX HEK293T cell line was employed for viral particles packaging (Clontech, Takara, Japan). Cells were maintained and expanded according to the vendor's suggestions. Primary human monocytes were

isolated from human blood as described previously, and GM-CSF-mediated differentiation was achieved also as described (Cushing et al., 2017; Primiano et al., 2016). These cells were stored at −80 °C.

2.3. Knockdown (KD)

All shRNA plasmids used for KD generation were designed by transOMIC Technologies (Huntsville, AL) based on the shERWOOD algorithm (Knott et al., 2014). Three different sequences were used for each tested genes – ABCb7, ABCb10, NLRP3 and VDAC1 plus a non-targeted sequence as control. Table 1 in Supplementary Material summaries the specific sequences used in this study. The link to the detailed descriptions of the transOMIC algorithm is below:

http://www.transomic.com/Products/RNAi/shERWOOD-UltramiR-shRNA/shERWOOD-Algorithm-Overview.aspx

HEK293T LentiX cells at 1×10^6 cells/well in 3 ml media were plated on 6-well tissue culture plates coated with poly-D-lysine and incubated overnight at 37 °C. The media was then exchanged and cells were rested at 37 °C for several hours prior to transfections. Transfection cocktails were prepared in 1.5 ml tubes containing 0.5 μg VSV-G and 1.5 μg PAX packaging plasmids plus 2 μg gene-specific shRNA lentiviral plasmids. 250 μl OptiMem was added to the DNA mixture, followed by addition of 12 μl of TransIT-LT1 transfection reagent (3 μl per 1 μg DNA). Transfection cocktails were slowly dropped on the HEK293T cells and plates were incubated overnight at 37 °C. Media from HEK293T cells was then removed and replaced with 3 ml of fresh HEK293T media and incubated an additional 24 h for virus production. The following day THP1 cells were seeded in 24- or 96-well-plates (2×10^6 in 0.5 ml, or 1×10^5 in 100 μl, respectively) in complete media. On that same day virus-containing media from HEK293T cells was supplemented with 2× polybrene concentrations and added at 0.5 ml/24-well or 100 μl/96-well on the THP1 cells. Cells were centrifuged at 2000 rpm for 2 h at 35 °C, and then transferred at 37 °C for 3 days to allow for genomic insertion and GFP expression. After 3 days, transduced cells were harvested, transferred into fresh media, and GPF expression was confirmed by visual inspection of cells under a fluorescent microscope (EVOS FL, Life Technologies, Carlsbad, CA, USA) followed by quantitation with flow cytometry. Four days after transduction, the remaining cells were used for functional analysis. For each independent functional experiment, a fresh culture of low passage THP1 cells was transduced with lentivirus or was exposed to polybrene alone to prepare the mock control group. Using standard methods, in virus titration experiments a suitable multiplicity of infection (MOI) for THP1 cells was found to be 10:1 virus:cell.

2.4. Knockout (KO)

ABCB10 and NLRP3 knockout THP1 cell lines were generated using a CRISPR-Cas9 ribonucleoprotein (RNP) complex consisting of Cas9 protein (TrueCut V2, Thermo Fisher Scientific) and modified synthetic sgRNA (Synthego). CRISPR gRNAs were designed for each gene using the Benchling platform (https://benchling.com). Guides were selected that target a region of each gene common to all reported the abcbisoforms. Two gRNAs (GAAACACGGCACTGAGCCCT_AGG and TTGAGCC CGAACAAACCCAC_AGG) were designed to delete a portion of exon 2 and intron 2 of the *ABCb10* genomic locus. A single gRNA (CCATCTT AATGGGACTCACG_GGG) was designed to target exon 3 of the *NLRP3* gene. The RNP complex was created by adding 600 pmol Cas9 with 60 pmol sgRNA at RT for 10 min prior to electroporation. 5×10^5 THP1 cells were re-suspended in 100 μl Nucleofector solution V (Lonza Bioscience, Cat. VCA-1003) containing RNP complex. Electroporations were performed using program V-001 on the Amaxa Nucleofector. Following electroporation, cells were transferred to 24-well plates containing enriched media for cell expansion. Enriched media consisted of a 50:50 mix of complete growth media plus THP1 conditioned media, and was empirically determined to improve THP1 cell survival. Transfected pools were assessed for the percentage of KO cells after 2 weeks in culture using a custom TaqMan copy number assay (Applied Biosystems) designed to the region disrupted by indels created by the RNP cutting and non-homologous end joining (NHEJ). Pools showing high levels of KO cells were then dilution-plated into 96-well plates at a concentration of 0.5 cells/well. After 3–4 weeks clones recovered from the dilution plating were again evaluated using the TaqMan copy number assay, screening for clones that harbored complete KO. Putative *ABCB10* and *NLRP3* KO clones were evaluated using Sanger sequencing of a PCR product spanning the CRISPR-modified genomic region for each gene. From the sequence data, *ABCB10* and *NLRP3* KO THP1 clones were identified as containing indels that created a frameshift on each allele of the gene. THP1 cells contain 2 copies of the *NLRP3* gene and 3 copies of the *ABCB10* gene. The identified ABCb10 KO clones contain a 126 bp deletion in exon 2 and into intron 2 for all alleles, corresponding to chromosome location Chr1 229,549,175–229,549,300, assembly GRCh38/hg38. The identified NLRP3 KO clones contain either a 1 or 2 bp deletion in exon 3 of the NLRP3 gene, corresponding to chromosome location Chr 1 247,424,043-247,424,044, assembly GRCh38/hg38.

2.5. Flow cytometry analysis

Lentiviral transduction efficiency was quantified using flow cytometric analysis of triplicate infections. In the first round, THP1 cells were transduced with pZIP lentiviral vectors utilizing a hCMV, mCMV, hEF1a, mEF1a or SFFV promoter. The remaining studies were performed using the pZIP-SFFV for shRNA mediated target KD. THP1 cells were harvested 72 h after transduction by pipetting and then washed twice with calcium and magnesium-free PBS containing 2% fetal bovine serum. Cells were suspended in the same buffer containing the viability dye 7-AAD (BD Biosciences, Franklin Lakes, NJ, USA) which was added immediately before analysis as recommended by the manufacturer. Flow cytometry data was collected using a LSR Fortessa cytometer (BD Biosciences) calibrated daily with CST beads. FCS files were analyzed by FlowJo V10 software. FSC-H *vs* FSC-W and SSC-H *vs* SSC-W gating were used sequentially to select single cellular events, and non-viable cells were identified by a 7-AAD staining and excluded from the analysis. Transduction efficiency was determined by % GFP-positive cells as depicted in Fig. 2, and vector expression levels of those GFP-positive cells were evaluated by MFI.

2.6. Inflammasome activation and cell viability assessments

Inflammasome activation was assessed as described by Primiano et al. (Primiano et al., 2016). Briefly, THP1 cells were plated in RPMI without supplements either in 6-well plates (for western blotting analysis) at $1–2 \times 10^6$ cells/well, or in 96-well plates at 1×10^5 cells/well for IC_{50} determination. Cells were primed for 3 h with 1 μg/ml of LPS, followed by 1 h stimulation with 10 μg/ml (13.4 μM) of nigericin, 2 h stimulation with 2 mM ATP, or overnight treatment with 200 μg/ml mono-sodium urate crystals (MSU). CP-453,773 was added during the last 30 min of LPS priming, prior to the addition of inflammasome stimuli. After appropriate times of activation, plates were centrifuged at 15,000 rpm for 5 min, supernatants were collected for cytokine analyses and cells were lysed for immunoblot analysis. Cytokine levels in media were assessed on a Meso Scale Discovery (MSD) platform. For immunoblot determination of processed IL-1β levels, Amicon Ultra-0.5 Centrifugal Filter Devices-10 K was used, according to the manufacturer's instructions. In brief, 0.5 ml of conditioned media was loaded onto the columns, centrifuged at 14,000 ×*g* for 20 min to achieve about 25-fold concentration. The ultrafiltrates were stored at −80 °C. Lactate dehydrogenase (LDH) release into the media was measured in fresh cell supernatants using a cytotoxicity detection kit (LDH) according to the manufacturer's instructions. 30 min incubation provided the best signal-to-noise ratio; absorbance at 490 nm was detected using a VersaMax

spectrophotometer (Molecular Devices). Cell viability was determined based on ATP consumption levels using the CellTiter-Glo® Luminescent Assay. After media was removed for the cytokine assay, 100 µl/well of CellTiter-Glo® Reagent for 96-well plates was added to the remaining 100 µl media plus cells, then shaken for 10 min at RT, and luminescence levels were detected on the EnVision (Perkin Elmer) platform.

2.7. Immunoblotting

Western blotting was performed according to a standard Odyssey protocol using for LI-COR detection method (LI-COR Biosciences, Lincoln, NE). Briefly, cells were lysed in 6-well plate by adding 100 µl/well of RIPA buffer supplemented with protease and phosphatase inhibitors, then 100 µl per sample of 2× SDS Loading buffer was added. Samples were heated at 95 °C for 5 min and briefly centrifuged; 20 µl sample was loaded per lane on 4–20% Tris-Glycine SDS-PAGE gels (Cat#XP04202BOX, ThermoFisher). Proteins were then transferred onto nitrocellulose membranes using an iBlot device (Cat# IB21001, ThermoFisher). Membranes were blocked in 20 ml of Odyssey blocking buffer (LiCor) for 1 h at RT. All primary antibodies were added at a 1:1000 dilution in 10 ml of Odyssey blocking buffer and incubated overnight at 4 °C, with the exception of anti-actin antibodies which were added at 1:2000 dilution. Membranes then were washed 3 × 10 min with TBST, incubated with the appropriate target species secondary antibody at 1:10,000 for 1 h at RT in the dark, followed by an additional 3 washes. Immuno-reactive bands were imaged using the Odyssey CLx and associated LI-COR software.

2.8. Statistical analyses and IC_{50} calculations

All values are expressed in the Figures as mean ± SEM. Statistical analysis between two variables was done using Welch's *t*-test and between groups with one-way ANOVA. In all Figures the following representations for *p* values were used: $p < .05$ = one asterisk (*); $p < .01$ = two asterisks (**); $p < .001$ = three asterisks (***); and $p < .0001$ = four asterisks (****). For IC50 calculations we used a log (agonist) *vs* response with a variable slope (four parameters) fit, with the following equation: Y = Bottom + (Top-Bottom)/(1 + 10^((LogEC50-X)*HillSlope) in GraphPad Prizm.

3. Results

3.1. Undifferentiated THP1 cells are a reliable cellular model for studying NLRP3 inflammasome activation

NLRP3 inflammasome activation occurs in undifferentiated THP1 cells in response to canonical NLRP3 pathway stimuli: treatments with nigericin, extracellular ATP, or MSU crystals induced IL-1β release from LPS-primed THP1 cells (4.52 ± 0.5 ng/ml, 2.20 ± 0.19 ng/ml, 2.46 ± 0.06 ng/ml, respectively; Fig. 1A). Of note, THP1 cells consistently release low, albeit detectable levels of IL-1β after stimulation with LPS alone (0.18 ± 0.07 ng/ml, across 4 independent experiments). Compared with LPS + ATP and LPS + MSU, LPS + nigericin induced the greatest increase in IL-1β release (Fig. 1A). Stimulation of THP1 cells with LPS alone or with any of these secondary stimuli alone did not result in IL-1β release into the culture media when measured by ELISA. LPS induction of TNFα (1.69 ± 0.2 ng/ml, Fig. 1A) was largely unaffected by additional stimulation with these NLRP3 inflammasome secondary stimuli. Undifferentiated THP1 cells stimulated with LPS + nigericin also released low but clearly detectable amounts of IL-18 (37.9 ± 3.75 pg/ml, not shown).

Undifferentiated THP1 cells are sensitive to CP-453,773 treatment. Pretreatment with CP-453,773 inhibited IL-1β release in a concentration-dependent manner with IC_{50}s of 47 nM and 56 nM for LPS + nigericin and LPS + MSU, respectively (Fig. 1B, Fig. S1A). The similarity in IC_{50} values for CP-453,773 inhibition of LPS + nigericin- and LPS + MSU-induced IL-1β suggests an identical mechanism of action of the drug under these two stimulation conditions, regardless of the particular NLRP3 inflammasome stimulus. As predicted, CP-453,773 did not inhibit TNFα release by THP1 cells under these conditions (Fig. 1B, Fig. S1A).

Activation of the NLRP3 inflammasome can lead to inflammasome-specific cell death known as pyroptosis (Fink and Cookson, 2005; Liu and Lieberman, 2017). Detection of lactate dehydrogenase (LDH) in the media is a sign of compromised cell membrane integrity and serves as an indicator of pyroptosis. In LPS-primed, nigericin-stimulated THP1 cells, CP-453,773 inhibited pyroptosis in a dose-dependent manner (Fig. S1B). The IC_{50} for inhibition of LDH release into the culture media (46 nM) was the same as the IC_{50} for the inhibition of IL-1β production. To further characterize NLRP3 inflammasome activation in undifferentiated THP1 cells we demonstrated the induction of pro-IL-1β and its processing in the culture media. THP1 cells were primed with LPS and then treated with nigericin, ATP or MSU, and cell lysates and conditioned media were collected and subjected to immunoblot analyses. Each secondary stimulus alone did not induce mature IL-1β in lysates or media, though LPS priming alone did induce pro-IL-1β. LPS priming followed by each of these secondary inflammasome stimuli caused processing of pro-IL-1β and IL-1β release in THP1 culture media (Fig. 1C, Fig. S1C) and cleavage of pro-caspase 1 to caspase 1 (Fig. S1C). In addition, while characterizing NLRP3 inflammasome components in THP1 cells we noticed significant differences in NLRP3 protein expression among various human cell types. In primary human monocytes and macrophages LPS priming is required for the expression of both NLRP3 and pro-IL-1β protein (prior to activation by a second signal). However, in undifferentiated THP1 cells NLRP3 protein is constitutively expressed, LPS priming is not necessary for the induction of NLRP3 protein, and LPS priming is only required for the induction of pro-IL-1β (Fig. 1D).

3.2. Optimization of specific and complete gene KD in THP1 cells

THP1 cells, like primary monocytes, can be challenging cells to virally transduce. We optimized a protocol to achieve reproducible transduction with high efficiency and viability using lentiviral constructs. The key findings are summarized in the Fig. 2. Using five different GFP reporter constructs, we found that the addition of centripetal force (spinfection) for 2 h considerably increased the percentage of GFP-expressing THP1 cells (Fig. 2A). The construct containing a spleen focus forming virus (SFFV) promoter yielded the highest percentage of transduced cells (95%) compared to human and mouse cytomegalovirus (hCMV and hCMV) and human and mouse elongation factor (hEF1a and mEF1a) promoters. Moreover, the SFFV promoter-containing construct yielded the brightest mean fluorescence intensity (MFI) by GFP expression (Fig. 2A) and was selected to generate constructs for subsequent gene-specific KDs. In pilot testing, we found that the addition of the cationic polymer polybrene to the THP1 cells prior to spinfection significantly improved the generation of GFP-expressing cells (not shown). All further transduction studies were carried out utilizing the spinfection method in the presence of polybrene.

To validate gene knockdown using the optimized transfection system in undifferentiated THP1 cells, we generated KD of NLRP3, ABCb7, ABCb10 and voltage-dependent anion-selective channel 1 (VDAC1). NLRP3 KD served as a positive control for inhibition of NLRP3 inflammasome activation. The ABCb7 and ABCb10 mitochondrial transporters were chosen for their plausible involvement in NLRP3 inflammasome activation based on the similitude of the glyburide and CP-453,773 structures. VDAC1 was chosen based on its published role in NLRP3 inflammasome activation (Zhou et al., 2011). All lentiviral plasmids were designed to express GFP and shRNA from distinct promoters, and all contained a puromycin resistance gene. To maintain KD cell populations and to avoid reversion to the wild-type phenotype, puromycin was added to the culture media as a selective pressure. In

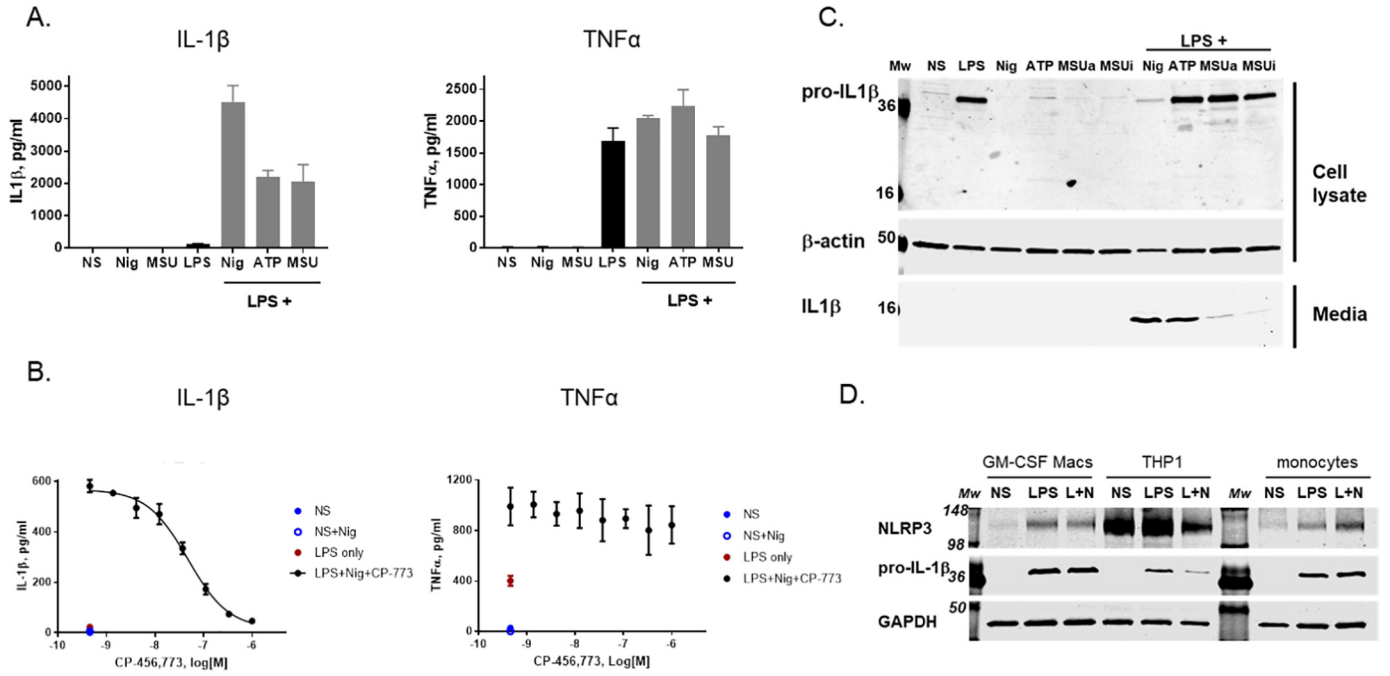

Fig. 1. Undifferentiated THP1 cells are a reliable cellular model for studying NLRP3 inflammasome activation. A. IL-1β and TNFα release from human THP1 cells primed with 1 μg/ml LPS for 3 h and then stimulated with 10 μg/ml nigericin for 1 h. Bars represent mean ± SEM (data shown are from three independent experiments with 4 technical replicates each). B. Effect of CP-456,774 on IL-1β and TNFα release from human THP1 cells primed with 1 μg/ml LPS for 3 h and then stimulated with 10 μg/ml nigericin for 1 h (data shown are from five independent experiments, with 3 technical replicates each). C. IL-1β processing after NLRP3 inflammasome activation in human THP1 cells: cells were primed with 1 μg/ml LPS for 3 h and then stimulated with 10 μg/ml nigericin for 1 h, or 2 mM ATP for 2 h, or 200 μg/ml MSU overnight (MSUa from AdipoGen, MSUi from InvivoGen). Immunoblots are representative of 3 independent experiments. D. NLRP3 protein expression before and after NLRP3 inflammasome activation in primary human monocytes-derived macrophages (GM-CSF Macs), undifferentiated THP1 cells and human primary monocytes. Immunoblots are representative of 3 independent experiments.

standard antibiotic killing assays, 1 μg/ml of puromycin was determined to be the optimal concentration for future experiments (Fig. S2A). For each target gene three distinct shRNA constructs were tested. Transduction efficiencies for all of these shRNAs and a non-targeting control shRNA were over 90% based on GFP expression (Fig. 2B). We also confirmed mRNA expression of several relevant genes, including the ATP receptor P2X7 (Fig. S2B). Fluorescence microscopy images confirmed expression of GFP in all transduced cells, and representative images for each transduced shRNA construct are provided in Fig. 2B, lower panel. ABCb7, ABCb10, VDAC1 and NLRP3 mRNA KD efficiencies were validated by evaluating the disruption of mRNA expression *via* quantitative RT-PCR. All lentiviral constructs resulted in significant reduction in mRNA levels for the intended target gene (Fig. 2C).

3.3. Evaluation of NLRP3 inflammasome activation following KDs

We tested our THP1 KD system for NLRP3 inflammasome activation. Priming cells with LPS did not noticeably change cell viability among all KDs tested, as judged by the CellTiter-Glo® Luminescent Cell Viability Assay. This assay quantifies cellular (lysate) ATP levels as a proxy for the amount of viable and metabolically active cells. As shown in Fig. 3A, activation of the NLRP3 inflammasome with LPS + nigericin considerably reduced cell viability. The absence of NLPR3 protected the cells against this inflammasome-mediated decrease in cell viability, while the absence of ABCb7 or ABCb10 did not. Under these conditions VDAC1 KD cells showed a viability that was similar to THP1 cells transduced with non-targeted shRNA or the mock-transduced controls (Fig. S3A).

As expected, NLPR3 KD in THP1 cells abolished IL-1β release into the media, similar to the published effect in the *NLRP3* KO mouse macrophages (Chen et al., 2016; Coll et al., 2015) (Fig. 3B). Deficiency in ABCb7 or ABCb10 did not alter IL-1β release in THP1 cells, relative to wild-type controls (Fig. 3B). Stimulation of virally transduced THP1 cells with LPS alone resulted in a minimal increase in IL-1β release of 0.04 ± 0.02 ng/ml across all 12 shRNAs. TNFα levels were not significantly altered in ABCb7 KD, ABCB10 KD, or NLRP3 KD THP1 cells (Fig. S3B). Interestingly, under these conditions VDAC1 was dispensable for NLRP3 inflammasome activation, in contrast to previously published results with THP1-derived macrophages (Fig. 3F) (Zhou et al., 2011).

To confirm the validity of our results with gene KD in THP1 cells, we chose to generate *ABCb7*, *ABCb10* and *NLRP3* knockout (KO) THP1 cell lines using a CRISPR/CAS9 transfection-based approach (see *Materials and Methods*). Briefly, for ABCb10 two different CRISPR guides (#1 and #2) were introduced into THP1 cells together by transfection, while for NLRP3 and ABCb7 a single CRISPR guide was used. From the *ABCb7* gRNA #1 plates, a total of 62 clones were obtained, and *ABCb7* gRNA #2 cloning resulted in 75 clones. This cycle of transfection/selection process was completed twice for ABCb7. DNA sequencing of clones from both guides revealed that all the clones that had any genomic modification had nucleotide deletions in factors of 3, which would not disrupt the reading frame. This finding suggests that *ABCb7* is likely an essential gene in THP1 cells, as the only cells that survived had this silent genomic modification. For *ABCb10*, 33 out of the 95 clones for gRNA #1 and 27 out of 86 clones for gRNA #2 showed complete KO of the gene at the genomic level. Viable *ABCb10* KO clones were confirmed by gene sequencing. *NLRP3* KO was developed based on 105 total positive clones from two gRNA and was validated by sequencing and by immunoblot analysis (Fig. S3D). In NLRP3 inflammasome activation assays the *ABCb10* KO clones had phenotypes comparable to wild type THP1 cells, similar to our results with ABCb10 KD cells. *ABCb10* KO clones were able to process IL-1β in response to NLRP3 inflammasome stimuli, and they produced levels of IL-1β in the media

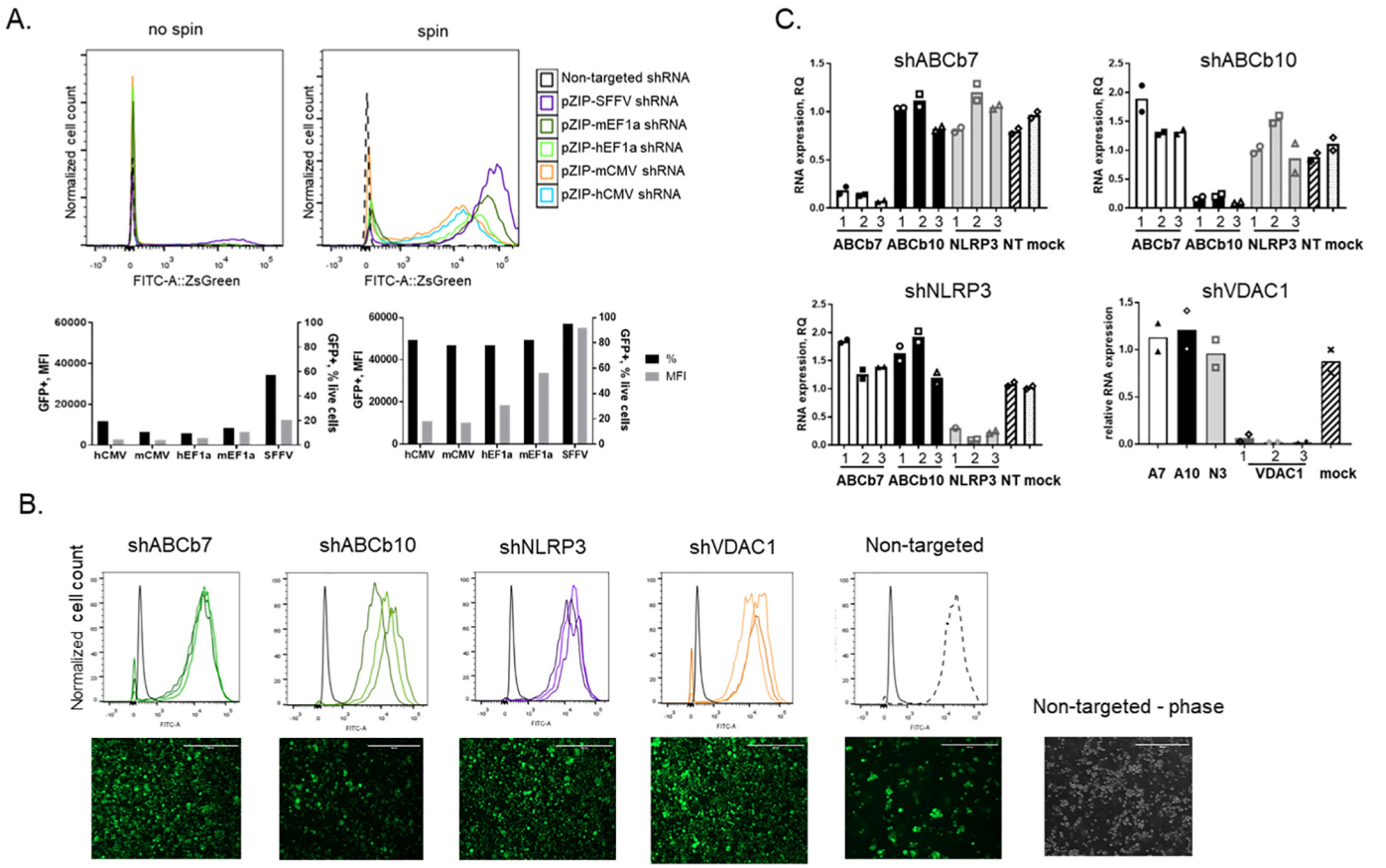

Fig. 2. Optimization of specific and complete gene KD in undifferentiated THP1 cells. A. Flow cytometry histograms of GFP expression in THP1 cells exposed to shRNA viral particles with or without spinfection by centrifugation for 2 h at 35 °C and analyzed for GFP expression. Data shown are from 1 of 2 experiments. Graph shows quantification of the above FACS histograms with and without spinfection with 5 different promoter constructs used to transduce THP1 cells. Bars represent normalized MFI and % GFP-positive THP1 cells. B. FACS analysis of constructs co-expressing GFP and 3 different shRNA for each target gene, plus control non-targeted (NT) shRNA. Flow cytometry for GFP expression was performed 3 days after viral infection. Representative images are shown for 1 of 3 shRNA constructs for each gene. C. Real-time qPCR analysis of gene expression in THP1 cells after spinfection using 3 different shRNA for each of ABCb7, ABCb10, and NLRP3 or NT shRNA; *1, 2* and *3* are different shRNA for each gene. Single data points represent independent transfections. Results shown are representative of 5 independent experiments.

that were similar to those from wild-type THP1 control cells (0.44 ± 0.03 ng/ml and 0.53 ± 0.04 ng/ml *vs.* 0.41 ± 0.04 ng/ml, respectively; Fig. 3C). Levels of TNFα were also comparable between wild-type THP1 and *ABCb10* KO THP1 (1.88 ± 0.05 ng/ml and 1.49 ± 0.10; 2.38 ± 0.23 ng/ml respectively; Fig. S3C). The *NLRP3* KO clones exhibited a complete blockade in IL-1β processing and release into the media. These IL-1β release results were consistent with the profile of pro-IL-1β expression in cell lysates, such that the disappearance of pro-IL-1β due to its processing to the mature form was blocked in the *NLRP3* KO clones (Fig. 3E). Altogether, the results generated with *ABCb10* and *NLRP3* KO clones supported our observations in shRNA KD cells that ABCb10 is dispensable for NLRP3 inflammasome activation and IL-1β release.

Given the fact that undifferentiated THP1 cells constitutively express NLRP3 protein, we investigated the possibility that pyroptosis could be induced in our model in the absence of LPS priming. We previously reported that treatment of primary mouse BMDMs with nigericin alone did not induce pyroptosis (Primiano et al., 2016). In undifferentiated THP1 cells, nigericin exposure alone, in the absence of LPS priming was capable of inducing pyroptotic cell death (Fig. 3E). To assess whether this effect was dependent on NLRP3, we exposed *NLRP3* KO clones to nigericin alone. *NLRP3* KO cells were completely protected from nigericin-induced loss of viability and increase in pyroptosis (Fig. 3F, CellTiter-Glo® lysate ATP levels, and LDH release, respectively). Given that nigericin treatment alone decreased cell viability, as indicated by LDH release and CellTiter-Glo® methodologies, we also investigated caspase-1 activation in THP1 cells exposed to nigericin. Under these conditions of nigericin-alone treatment, pro-caspase-1 was cleaved and fully processed caspase-1 was produced (Fig. S3F). This finding highlights a unique advantage of the undifferentiated THP1 cell system inasmuch as the NLRP3 inflammasome can be activated in the absence of LPS priming, thereby enabling the study of cellular processes induced by second signals such as nigericin, but in the absence of confounding cellular responses to the LPS-mediated priming signal.

3.4. Investigation of putative CP-453,773 pharmacologic targets in undifferentiated THP1 cells

ABCb7 and ABCb10 KD lines produced levels of IL-1β in the media that were similar to IL-1β levels in non-targeted- and mock-shRNA transduced THP1 cell cultures (~0.2 ng/ml), while IL-1β protein expression from NLRP3 KD THP1 cells was significantly reduced (Fig. 4A). Pre-incubation with CP-453,773 completely abolished the ability of cells to release processed IL-1β in ABCb7 and ABCb10 KD lines. These cells were phenotypically identical to the wild-type control cells with respect to CP-453,773 mediated inhibition of IL-1β release (Fig. 4A). TNFα release in ABCb7 or ABCb10 KD cells was also similar to the TNFα release profile of control THP1 cells (Fig. S4A).

To address the possibility that ABCb7 or ABCb10 antagonize inflammasome activation in a manner analogous to the function of SUR

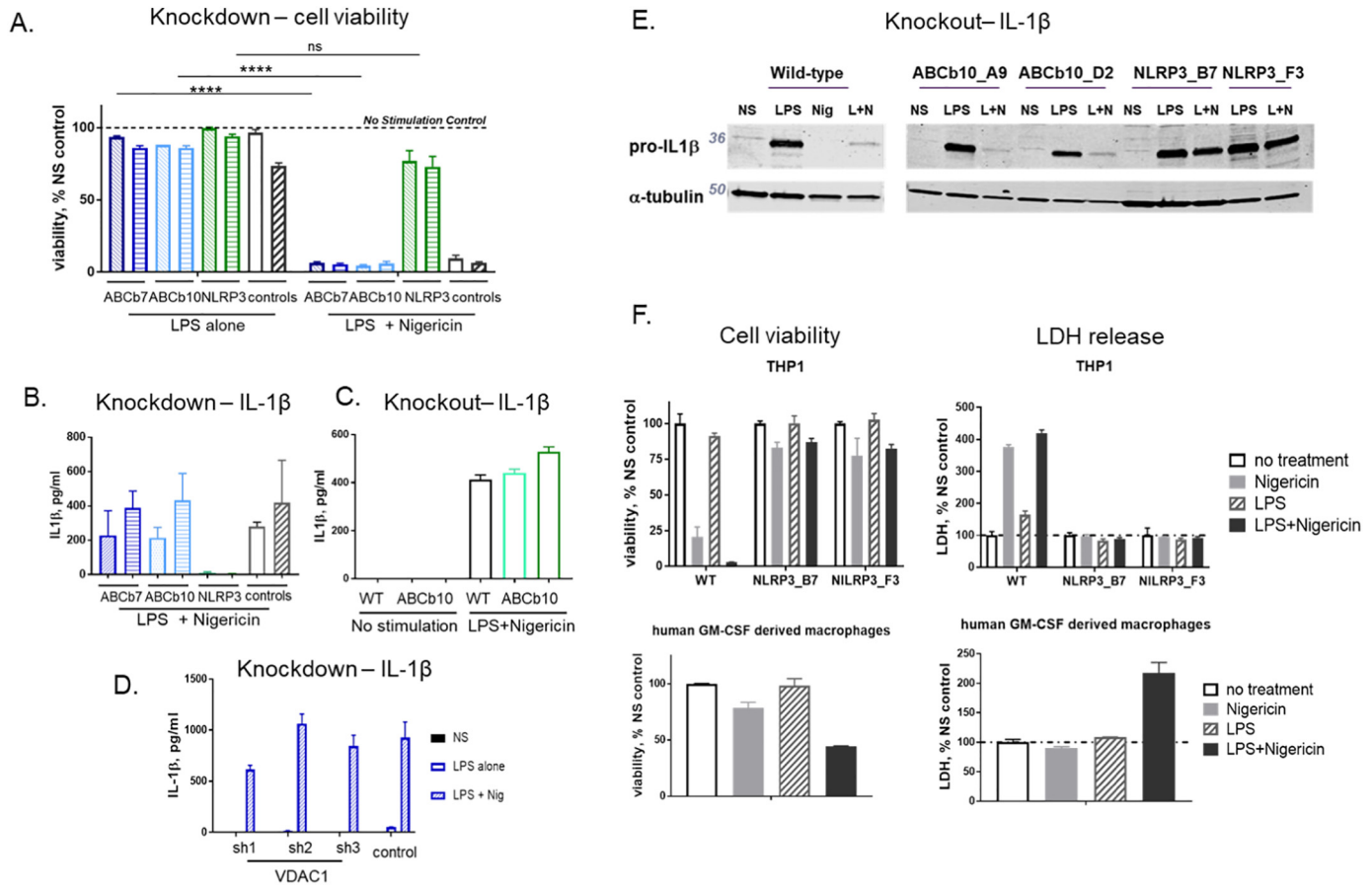

Fig. 3. Silencing of ABCb7 or ABCb10 does not change inflammasome activation. A. Viability of THP1 cells was measured 72 h post-transduction with shRNAs. Data shown are for 2 different shRNA for each gene. Controls were either mock (white bars) or non-transduced (black/white bars) THP1 cells. Statistical significance was determined by ANOVA for all sets and the unpaired student's *t*-test was used within the specific groups. Data shown are from 1 of 3 independent experiments; mean ± SEM of 4 technical replicates. B and C. IL-1β release from THP1 cells primed with 1 μg/ml LPS for 3 h and then stimulated with 10 μg/ml nigericin for 1 h. Results for ABCb7, ABCb10, NLRP3 and NT shRNA KDs are shown in *B* and results for *ABCb10* KO clones are shown in *C* (mean ± SEM of 3 independent experiments). D. IL-1β release from VDAC1 KD THP1 cells after cell treatment as in panel B. Representative data for 1 of 3 independent experiments; mean ± SEM of 4 technical replicates. E. Intracellular levels of IL-1β after NLRP3 inflammasome activation in wild-type THP1 and *ABCb10* (A9, D2) and *NLRP3* (B7, F3) KO clones. Images are representative of 3 independent experiments. E. Viability and LDH release in wild-type THP1 and *NLRP3* (B7, F3) KO clones, compared with primary human GM-CSF derived macrophages. Data shown are from 1 of 3 independent experiments; mean ± SEM of 4 technical replicates.

proteins on pancreatic β-cells, we tested whether the potency of CP-453,773 is 'right-shifted' in the absence of these transporters. If ABCb7 or ABCb10 antagonize NLRP3 inflammasome mediated IL-1β production, then the deletion of these gene products might be expected to decrease CP-453,773 potency, resulting in an increase in its IC_{50}. As shown in Fig. 4B, the IC_{50} of CP-453,773 for inhibition of IL-1β release was not significantly altered in ABCb7 or ABCb10 KD clones, relative to non-targeted shRNA control THP1 cells. These IC_{50} values were 11.3 ± 2.0 nM and 6.3 ± 0.4 nM for ABCb7 and ABCb10, respectively, and they were therefore not right-shifted relative to the IC_{50} of 25.5 ± 2.7 nM in non-targeted shRNA control THP1 cells. Confirming these shRNA KD results, CP-453,773 IC_{50} values for inhibition of IL-1β release into the culture media were also similar between *ABCb10* KO clones and wild-type THP1 cells (85.0 ± 63.3 nM, 54.2 ± 14.8 nM and 50.2 ± 24.3 nM for 2 ABCb10 KO clones and wild-type THP1, respectively) (Fig. 4C).

We also compared the processing of pro-IL-1β into IL-1β in *ABCb10* and *NLRP3* KO clones, in the presence/absence of CP-453,773. As shown in Fig. 4D, in wild-type THP1 cells, and in the *ABCb10* KO clones, treatment with LPS alone induced *de novo* expression of pro-IL-1β protein. Treatment of wild-type and *ABCb10* KO THP1 cells with LPS + nigericin induced both a reduction of pro-IL-1β protein in cell lysates and a simultaneous appearance of processed IL-1β in the culture media. Both of these effects were blocked by CP-453,773 in these cells, indicating that both are NLRP3-dependent mechanisms. Indeed, KO of *NLRP3* resulted in complete inhibition of the reduction in pro-IL-1β protein in cell lysates, and in the disappearance of fully processed IL-1β in the media, in response to LPS + nigericin stimulation. As expected, both of these effects were not altered by CP-453,773 in *NLRP3* KO cells (Fig. 4D, lower right panel). In addition, pro-Caspase-1 protein was constitutively expressed in wild-type and *ABCb10* KO THP1 cells, and cleavage of pro-Caspase-1 occurred in response to LPS + nigericin stimulation. This LPS + nigericin induced processing of pro-Caspase-1 in wild-type and *ABCb10* KO THP1 cells was blocked by CP-453,773. It was also blocked in the *NLRP3* KO THP1 cells.

Taken together, our results provide pharmacologic and genetic validation for the use of undifferentiated THP1 cells as a reproducible, relevant, and mechanistically accurate *in vitro* cellular system for studying NLRP3 inflammasome biology.

4. Discussion

IL-1β, a pyrogenic and inflammatory cytokine, has been studied for many years due to its central role in inflammation (Yu and Lee, 2016). IL-1β is produced as a consequence of NLRP3 inflammasome activation, as well as among other inflammasomes, such as AIM2, NLRC4 or

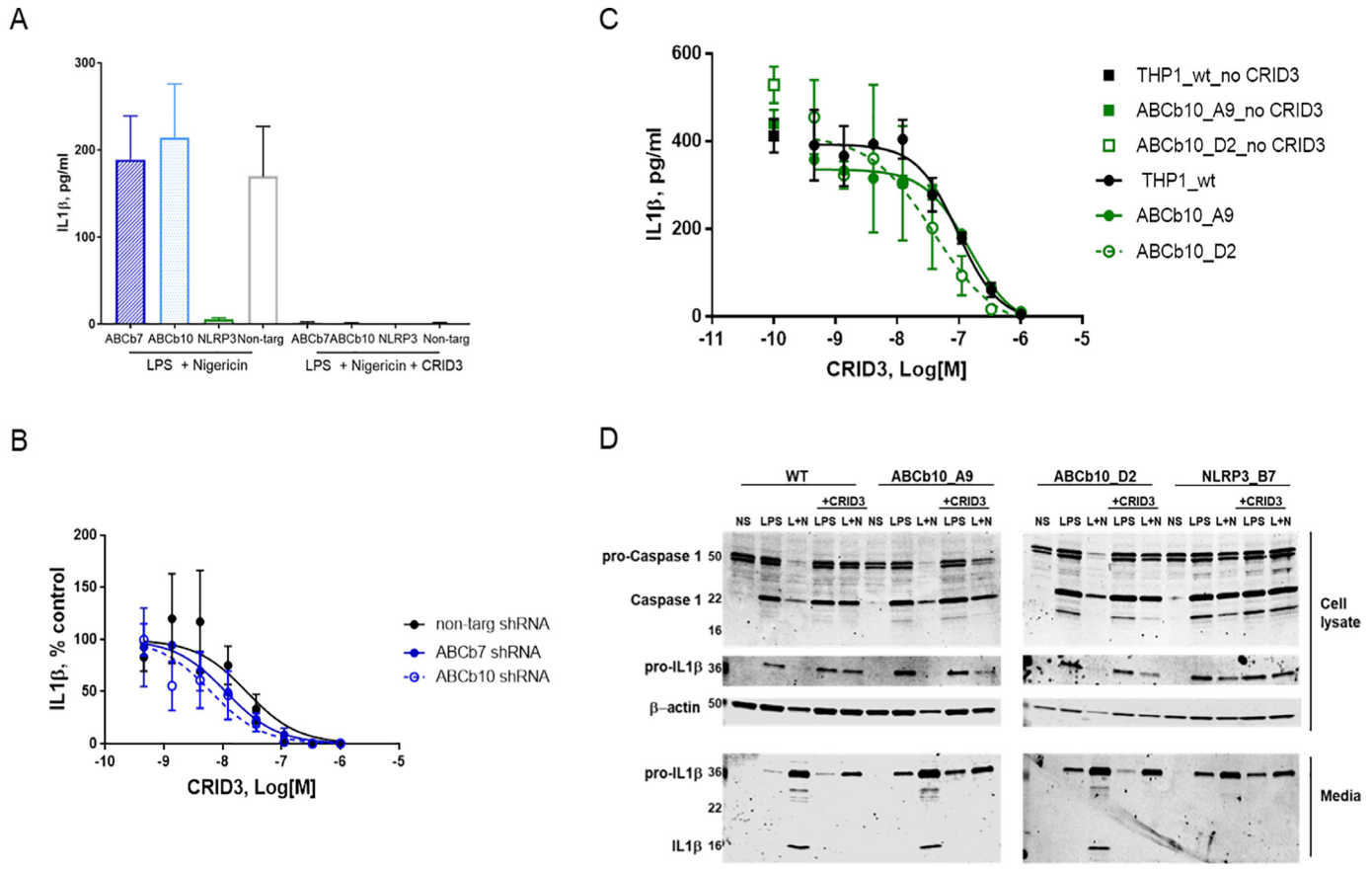

Fig. 4. Investigation of putative CP-453,773 pharmacologic targets in undifferentiated THP1 cells. A. IL-1β release from ABCb7, ABCb10 and NLRP3 KD THP1 cells primed with 1 μg/ml LPS for 3 h, then treated with 1 μM CP-453,773 for 30 min, and then stimulated with 10 μg/ml nigericin for 1 h (n = 3). B. IL-1β inhibition in ABCb7 and ABCb10 KD THP1 cells primed with 1 μg/ml LPS for 3 h, then treated with 1 μM CP-453,773 for 30 min, and then stimulated with 10 μg/ml nigericin for 1 h (n = 3). C. IL-1β inhibition in *ABCb10* (A9, D2) KO THP1 cells primed with 1 μg/ml LPS for 3 h, then treated with 1 μM CP-453,773 for 30 min, and then stimulated with 10 μg/ml nigericin for 1 h (n = 3). D. Pro-IL-1β and pro-caspase-1 processing after NLRP3 inflammasome activation in THP1 KO cells: cells were primed with 1 μg/ml LPS for 3 h and then stimulated with 10 μg/ml nigericin for 1 h. Images are representative of 3 independent experiments.

NLRP1, during the response to a multitude of cellular stresses. We optimized the undifferentiated THP1 cell system to better characterize both the NLRP3 pathway itself in this system and the roles of putative NLRP3 pathway component proteins. We employed this THP1 model system to test the hypothesis that the mitochondrial transporters ABCb7 and ABCb10 are pharmacologic targets(s) of CP-453,773, a selective small molecule inhibitor of NLRP3-dependent IL-1β production.

Activation of the NLRP3 inflammasome has been demonstrated in PMA-differentiated, macrophage-like THP1 cells, but considering recent reports of possible differences between monocyte and macrophage responses to inflammasome stimuli (Gaidt et al., 2016), we chose to use undifferentiated THP1 cells. These cells are non-adherent (suspension) and proliferative, which greatly facilitates their use and maintenance and inter-experimental consistency. Priming with LPS followed by the application of secondary triggers such as ATP, nigericin, or MSU crystals induced CP-453,773-sensitive IL-1β production and pyroptosis, highlighting the fact that the pharmacologic target of CP-453,773 is present in undifferentiated THP1 cells. Using lentivirally-delivered shRNA, selecting an optimal promoter to drive transgene expression, and adding a spinfection step to the transduction protocol, we developed a reproducible method for gene KD in undifferentiated THP1 cells. > 90% of viable cells expressed vector-encoded GFP protein, indicating high transduction efficiencies, and shRNA-mediated reductions in mRNA expression of > 90% was achieved for all targets.

Our examination of whether the mitochondrial transporters ABCb7 or ABCb10 are uniquely involved in NLRP3 inflammasome activation and are pharmacologic targets of CP-453,773 was based on the following: 1) the known mechanism-of-action of glyburide, and its targeting of the ABC transporters SUR1, SUR2a and SUR2b on pancreatic β-cells (Lamkanfi et al., 2009), 2) the fact that both CP-453,773 and glyburide are highly related sulfonyl-urea-based drugs (Laliberte et al., 2003), 3) the selectivity of CP-453,773 for inhibition of the NLRP3 inflammasome (Primiano et al., 2016; Coll et al., 2015), and 4) the critical role for mitochondria in NLRP3 inflammasome activation and the mitochondria-restricted expression of ABCb7 and ABCb10 (Gurung et al., 2015; Heid et al., 2013; Iyer et al., 2013; Yu and Lee, 2016; Shimada et al., 1998; Liesa et al., 2012). In ABCb7- and ABCb10-deficient THP1 cells, however, inflammasome activation was unaffected, the efficacy of CP-453,773 for inhibition of IL-1β release in response to NLRP3 stimuli was not altered, and the IC_{50} of CP-453,773 for inhibition of IL-1β release was not increased. Moreover, by analogy with the mechanism-of-action of glyburide, we suspected that if the target of CP-453,773 *agonizes* a mitochondrial *antagonist* of NLRP3 activation, then the removal of such a target should cause an *increase* in IL-1β release. However, in response to NLRP3-specific stimuli the amount of IL-1β released from ABCb7 and ABCb10 KD THP1 cells was indistinguishable from IL-1β release in non-targeted shRNA control (wild-type) THP1 cells. Therefore, we conclude that the ABCb7 and ABCb10 mitochondrial transporters are not the pharmacologic targets of CP-453,773.

Both ABCb7 and ABCb10 have been reported to be involved in iron transport, metabolism and homeostasis (Bekri et al., 2000; Hyde et al., 2012; Yamamoto et al., 2014). The precise biological role and function of ABCb10 remains unclear; however, deletion of the *ABCb10* gene is

lethal in mice due to a detrimental defect in heme synthesis (Yamamoto et al., 2014). In a human liver cell line, silencing of ABCb10 caused a reduction in the unfolded protein response in mitochondria (Yano, 2017). The ABC KD and KO cell lines developed as part of the present work will facilitate further exploration of their role in iron homeostasis, cellular metabolism, and mitochondrial function.

In summary, we demonstrated that undifferentiated THP1 cells can be utilized as a reliable and simplified model for studying NLRP3 inflammasome. The results presented herein have allowed us to reject the possibility that ABCb7 and ABCb10 are pharmacologic targets of CP-453,773. We anticipate that further studies of the NLRP3 inflammasome using undifferentiated THP1 cells will reveal both the target of CP-453,773 and novel targets within the NLRP3 inflammasome pathway.

Conflict of interest

The authors do not have any conflicts of interest to declare.

Acknowledgements

The authors wish to thank Dr. Samantha Hiemer for providing initial insights on lentivirus KD approaches, Dr. Joe Brennan for editing assistance, and Dr. Tom Wynn for helpful suggestions.

Appendix A. Supplementary data

Supplementary data to this article can be found online at https://doi.org/10.1016/j.jim.2019.02.002.

References

Adati, N., Huang, M.C., Suzuki, T., Suzuki, H., Kojima, T., 2009. High-resolution analysis of aberrant regions in autosomal chromosomes in human leukemia THP-1 cell line. BMC Res. Notes 2, 153.

Bekri, S., Kispal, G., Lange, H., Fitzsimons, E., Tolmie, J., Lill, R., Bishop, D.F., 2000. Human ABC7 transporter: gene structure and mutation causing X-linked sideroblastic anemia with ataxia with disruption of cytosolic iron-sulfur protein maturation. Blood 96, 3256–3264.

Berman, N., Dunham, J., Vivino, F., 2014. Cryopyrin-associated periodic fever syndrome presenting with fevers and serositis related to a novel NLRP3 gene mutation. J. Clin. Rheumatol. 20, 451–452.

Buscher, K., Ehinger, E., Gupta, P., Pramod, A.B., Wolf, D., Tweet, G., Pan, C., Mills, C.D., Lusis, A.J., Ley, K., 2017. Natural variation of macrophage activation as disease-relevant phenotype predictive of inflammation and cancer survival. Nat. Commun. 8, 16041.

Cante-Barrett, K., Mendes, R.D., Smits, W.K., Van Helsdingen-Van Wijk, Y.M., Pieters, R., Meijerink, J.P., 2016. Lentiviral gene transfer into human and murine hematopoietic stem cells: size matters. BMC Res. Notes 9, 312.

Chavarria-Smith, J., Vance, R.E., 2015. The NLRP1 inflammasomes. Immunol. Rev. 265, 22–34.

Chen, K., Shanmugam, N.K., Pazos, M.A., Hurley, B.P., Cherayil, B.J., 2016. Commensal bacteria-induced inflammasome activation in mouse and human macrophages is dependent on potassium efflux but does not require phagocytosis or bacterial viability. PLoS One 11, e0160937.

Coll, R.C., Robertson, A.A., Chae, J.J., Higgins, S.C., Munoz-Planillo, R., Inserra, M.C., Vetter, I., Dungan, L.S., Monks, B.G., Stutz, A., Croker, D.E., Butler, M.S., Haneklaus, M., Sutton, C.E., Nunez, G., Latz, E., Kastner, D.L., Mills, K.H., Masters, S.L., Schroder, K., Cooper, M.A., O'neill, L.A., 2015. A small-molecule inhibitor of the NLRP3 inflammasome for the treatment of inflammatory diseases. Nat. Med. 21, 248–255.

Cullen, S.P., Kearney, C.J., Clancy, D.M., Martin, S.J., 2015. Diverse activators of the NLRP3 inflammasome promote IL-1beta secretion by triggering necrosis. Cell Rep. 11, 1535–1548.

Cushing, L., Winkler, A., Jelinsky, S.A., Lee, K., Korver, W., Hawtin, R., Rao, V.R., Fleming, M., Lin, L.L., 2017. IRAK4 kinase activity controls Toll-like receptor-induced inflammation through the transcription factor IRF5 in primary human monocytes. J. Biol. Chem. 292, 18689–18698.

Dinarello, C.A., 2015. The history of fever, leukocytic pyrogen and interleukin-1. Temperature (Austin) 2, 8–16.

Duncan, J.A., Canna, S.W., 2018. The NLRC4 inflammasome. Immunol. Rev. 281, 115–123.

Dupont, N., Jiang, S., Pilli, M., Ornatowski, W., Bhattacharya, D., Deretic, V., 2011. Autophagy-based unconventional secretory pathway for extracellular delivery of IL-1beta. EMBO J. 30, 4701–4711.

Fink, S.L., Cookson, B.T., 2005. Apoptosis, pyroptosis, and necrosis: mechanistic description of dead and dying eukaryotic cells. Infect. Immun. 73, 1907–1916.

Franchi, L., Warner, N., Viani, K., Nunez, G., 2009. Function of Nod-like receptors in microbial recognition and host defense. Immunol. Rev. 227, 106–128.

Gaidt, M.M., Ebert, T.S., Chauhan, D., Schmidt, T., Schmid-Burgk, J.L., Rapino, F., Robertson, A.A., Cooper, M.A., Graf, T., Hornung, V., 2016. Human monocytes engage an alternative inflammasome pathway. Immunity 44, 833–846.

Gurung, P., Lukens, J.R., Kanneganti, T.D., 2015. Mitochondria: diversity in the regulation of the NLRP3 inflammasome. Trends Mol. Med. 21, 193–201.

He, Y., Hara, H., Nunez, G., 2016. Mechanism and regulation of NLRP3 inflammasome activation. Trends Biochem. Sci. 41, 1012–1021.

Heid, M.E., Keyel, P.A., Kamga, C., Shiva, S., Watkins, S.C., Salter, R.D., 2013. Mitochondrial reactive oxygen species induces NLRP3-dependent lysosomal damage and inflammasome activation. J. Immunol. 191, 5230–5238.

Hill, J.R., Coll, R.C., Sue, N., Reid, J.C., Dou, J., Holley, C.L., Pelingon, R., Dickinson, J.B., Biden, T.J., Schroder, K., Cooper, M.A., Robertson, A.A.B., 2017. Sulfonylureas as concomitant insulin secretagogues and nlrp3 inflammasome inhibitors. ChemMedChem 12, 1449–1457.

Horvath, G.L., Schrum, J.E., De Nardo, C.M., Latz, E., 2011. Intracellular sensing of microbes and danger signals by the inflammasomes. Immunol. Rev. 243, 119–135.

Hyde, B.B., Liesa, M., Elorza, A.A., Qiu, W., Haigh, S.E., Richey, L., Mikkola, H.K., Schlaeger, T.M., Shirihai, O.S., 2012. The mitochondrial transporter ABC-me (ABCB10), a downstream target of GATA-1, is essential for erythropoiesis in vivo. Cell Death Differ. 19, 1117–1126.

Iyer, S.S., He, Q., Janczy, J.R., Elliott, E.I., Zhong, Z., Olivier, A.K., Sadler, J.J., Knepper-Adrian, V., Han, R., Qiao, L., Eisenbarth, S.C., Nauseef, W.M., Cassel, S.L., Sutterwala, F.S., 2013. Mitochondrial cardiolipin is required for Nlrp3 inflammasome activation. Immunity 39, 311–323.

Kim, J.H., Sohn, H.J., Yoo, J.K., Kang, H., Seong, G.S., Chwae, Y.J., Kim, K., Park, S., Shin, H.J., 2016. NLRP3 inflammasome activation in THP-1 target cells triggered by pathogenic Naegleria fowleri. Infect. Immun. 84, 2422–2428.

Knott, S., Maceli, A., Erard, N., Chang, K., Marran, K., Zhou, X., Gordon, A., Demerdash, O., Wagenblast, E., Kim, S., Fellmann, C., Hannon, G., 2014. A Computational Algorithm to Predict shRNA Potency. Mol. Cell 56, 796–807.

Laliberte, R.E., Perregaux, D.G., Hoth, L.R., Rosner, P.J., Jordan, C.K., Peese, K.M., Eggler, J.F., Dombroski, M.A., Geoghegan, K.F., Gabel, C.A., 2003. Glutathione s-transferase omega 1-1 is a target of cytokine release inhibitory drugs and may be responsible for their effect on interleukin-1beta posttranslational processing. J. Biol. Chem. 278, 16567–16578.

Lamkanfi, M., Mueller, J.L., Vitari, A.C., Misaghi, S., Fedorova, A., Deshayes, K., Lee, W.P., Hoffman, H.M., Dixit, V.M., 2009. Glyburide inhibits the Cryopyrin/Nalp3 inflammasome. J. Cell Biol. 187, 61–70.

Liesa, M., Qiu, W., Shirihai, O.S., 2012. Mitochondrial ABC transporters function: the role of ABCB10 (ABC-me) as a novel player in cellular handling of reactive oxygen species. Biochim. Biophys. Acta 1823, 1945–1957.

Liu, X., Lieberman, J., 2017. How ICE lights the pyroptosis fire. Cell Death Differ. 24, 197–199.

Longo, D.M., Louie, B., Wang, E., Pos, Z., Marincola, F.M., Hawtin, R.E., Cesano, A., 2012. Inter-donor variation in cell subset specific immune signaling responses in healthy individuals. Am. J. Clin. Exp. Immunol. 1, 1–11.

Lopez-Castejon, G., Brough, D., 2011. Understanding the mechanism of IL-1beta secretion. Cytokine Growth Factor Rev. 22, 189–195.

Mukherjee, C., Hale, C., Mukhopadhyay, S., 2018. A simple multistep protocol for differentiating human induced pluripotent stem cells into functional macrophages. Methods Mol. Biol. 1784, 13–28.

Munoz-Planillo, R., Kuffa, P., Martinez-Colon, G., Smith, B.L., Rajendiran, T.M., Nunez, G., 2013. K(+) efflux is the common trigger of NLRP3 inflammasome activation by bacterial toxins and particulate matter. Immunity 38, 1142–1153.

Murakami, T., Ockinger, J., Yu, J., Byles, V., Mccoll, A., Hofer, A.M., Horng, T., 2012. Critical role for calcium mobilization in activation of the NLRP3 inflammasome. Proc. Natl. Acad. Sci. U. S. A. 109, 11282–11287.

Nagar, A., Demarco, R.A., Harton, J.A., 2018. Inflammasome and Caspase-1 activity characterization and evaluation: an imaging flow cytometer-based detection and assessment of inflammasome specks and Caspase-1 activation. J. Immunol. 202, 1003–1015.

Nakahira, K., Haspel, J.A., Rathinam, V.A., Lee, S.J., Dolinay, T., Lam, H.C., Englert, J.A., Rabinovitch, M., Cernadas, M., Kim, H.P., Fitzgerald, K.A., Ryter, S.W., Choi, A.M., 2011. Autophagy proteins regulate innate immune responses by inhibiting the release of mitochondrial DNA mediated by the NALP3 inflammasome. Nat. Immunol. 12, 222–230.

Nomura, J., So, A., Tamura, M., Busso, N., 2015. Intracellular ATP decrease mediates NLRP3 inflammasome activation upon nigericin and crystal stimulation. J. Immunol. 195, 5718–5724.

Perregaux, D., Barberia, J., Lanzetti, A.J., Geoghegan, K.F., Carty, T.J., Gabel, C.A., 1992. IL-1 beta maturation: evidence that mature cytokine formation can be induced specifically by nigericin. J. Immunol. 149, 1294–1303.

Perregaux, D.G., Mcniff, P., Laliberte, R., Hawryluk, N., Peurano, H., Stam, E., Eggler, J., Griffiths, R., Dombroski, M.A., Gabel, C.A., 2001. Identification and characterization of a novel class of interleukin-1 post-translational processing inhibitors. J. Pharmacol. Exp. Ther. 299, 187–197.

Piccioli, P., Rubartelli, A., 2013. The secretion of IL-1beta and options for release. Semin. Immunol. 25, 425–429.

Place, D.E., Kanneganti, T.D., 2018. Recent advances in inflammasome biology. Curr. Opin. Immunol. 50, 32–38.

Primiano, M.J., Lefker, B.A., Bowman, M.R., Bree, A.G., Hubeau, C., Bonin, P.D., Mangan, M., Dower, K., Monks, B.G., Cushing, L., Wang, S., Guzova, J., Jiao, A., Lin, L.L., Latz, E., Hepworth, D., Hall, J.P., 2016. Efficacy and pharmacology of the NLRP3 inflammasome inhibitor CP-456,773 (CRID3) in murine models of dermal and

pulmonary inflammation. J. Immunol. 197, 2421–2433.
Rathinam, V.A., Jiang, Z., Waggoner, S.N., Sharma, S., Cole, L.E., Waggoner, L., Vanaja, S.K., Monks, B.G., Ganesan, S., Latz, E., Hornung, V., Vogel, S.N., Szomolanyi-Tsuda, E., Fitzgerald, K.A., 2010. The AIM2 inflammasome is essential for host defense against cytosolic bacteria and DNA viruses. Nat. Immunol. 11, 395–402.
Schildberger, A., Rossmanith, E., Eichhorn, T., Strassl, K., Weber, V., 2013. Monocytes, peripheral blood mononuclear cells, and THP-1 cells exhibit different cytokine expression patterns following stimulation with lipopolysaccharide. Mediat. Inflamm. 2013, 697972.
Shimada, Y., Okuno, S., Kawai, A., Shinomiya, H., Saito, A., Suzuki, M., Omori, Y., Nishino, N., Kanemoto, N., Fujiwara, T., Horie, M., Takahashi, E., 1998. Cloning and chromosomal mapping of a novel ABC transporter gene (hABC7), a candidate for X-linked sideroblastic anemia with spinocerebellar ataxia. J. Hum. Genet. 43, 115–122.
Subramanian, N., Natarajan, K., Clatworthy, M.R., Wang, Z., Germain, R.N., 2013. The adaptor MAVS promotes NLRP3 mitochondrial localization and inflammasome activation. Cell 153, 348–361.
Vanaja, S.K., Rathinam, V.A., Fitzgerald, K.A., 2015. Mechanisms of inflammasome activation: recent advances and novel insights. Trends Cell Biol. 25, 308–315.
Wang, H., Mao, L., Meng, G., 2013. The NLRP3 inflammasome activation in human or mouse cells, sensitivity causes puzzle. Protein Cell 4, 565–568.
Yamamoto, M., Arimura, H., Fukushige, T., Minami, K., Nishizawa, Y., Tanimoto, A., Kanekura, T., Nakagawa, M., Akiyama, S., Furukawa, T., 2014. Abcb10 role in heme biosynthesis in vivo: Abcb10 knockout in mice causes anemia with protoporphyrin IX and iron accumulation. Mol. Cell. Biol. 34, 1077–1084.
Yano, M., 2017. ABCB10 depletion reduces unfolded protein response in mitochondria. Biochem. Biophys. Res. Commun. 486, 465–469.
Yu, J.W., Lee, M.S., 2016. Mitochondria and the NLRP3 inflammasome: physiological and pathological relevance. Arch. Pharm. Res. 39, 1503–1518.
Zhou, R., Yazdi, A.S., Menu, P., Tschopp, J., 2011. A role for mitochondria in NLRP3 inflammasome activation. Nature 469, 221–225.